The critical behaviour of Potts models with symmetry- breaking fields

1996 J. Phys. A: Math. Gen. 29 3329

(http://iopscience.iop.org/0305-4470/29/13/009)

J. Phys. A: Math. Gen. **29** (1996) 3329–3339. Printed in the UK

The critical behaviour of Potts models with symmetry-breaking fields

F C Alcaraz and J C Xavier
Departamento de Física, Universidade Federal de São Carlos, 13565-905, São Carlos, SP, Brazil

Received 31 October 1995, in final form 19 February 1996

Abstract. The Q-state Potts model in two dimensions in the presence of external magnetic fields is studied. For general $Q \geqslant 3$ special choices of these magnetic fields produce effective models with smaller $Z(Q')$ symmetry ($Q' < Q$). The phase diagram of these models and their critical behaviour are explored by conventional finite-size scaling and conformal invariance. The possibility of multicritical behaviour, for finite values of the symmetry-breaking fields, in the cases where $Q > 4$ is also analysed. Our results indicate that for effective models with $Z(Q')$ symmetry ($Q' \leqslant 4$) the multicritical point occurs at zero field. This last result is also corroborated by Monte Carlo simulations.

1. Introduction

The ferromagnetic Q-state Potts model in two dimensions is among the most studied models of statistical mechanics (see [1] for a review). In the absence of external fields the model has a global $Z(Q)$ invariance† which, for low temperatures, is spontaneously broken giving rise to phase transitions of second order for $Q \leqslant 4$ and first order for $Q > 4$ [2]. The critical fluctuations for $Q = 2, 3$ and 4 are governed by conformal field theories with central charges $c = \frac{1}{2}, \frac{4}{5}$ and 1, respectively, and the whole operator content of these models with several boundary conditions is known [3].

In this paper we study the critical behaviour of these models on the square lattice, in the presence of symmetry-breaking magnetic fields. In general, these fields will completely break the $Z(Q)$ symmetry, but for some special choices of these magnetic fields the resulting effective model will have a residual symmetry $Z(Q')$, with $Q' < Q$, and a domain wall structure at low temperatures, similar to these in the Q'-state Potts model.

On general grounds [4], we do expect that in order–disorder phase transitions, of discrete symmetry models, the critical behaviour is dictated mainly by the number of ground states (zero-temperature configurations) and the relative surface energy of the infinite domain walls connecting these ground states. This reasoning induces us to expect, for arbitrary values of the symmetry-breaking fields, producing a $Z(Q')$ model, an effective model in the same universality class as the Q'-state Potts model. However, this analysis is not valid in general since some critical and multicritical models, like the Ising model and the tricritical Ising model [5], although having the same number of ground states and domain wall structure at low temperatures, exhibit distinct critical properties.

Straley and Fisher [6] by series expansion in the $Q = 3$ model suggested that the $Z(2)$ model, produced by the breaking fields, is in the same universality class as the two-state

† Actually the model has a larger symmetry $S(Q)$, the permutation group of Q objects.

Potts model, for non-zero values of the fields. For values of $Q > 4$, with $Q' < 4$, the mean-field analysis [1, 6] indicate a multicritical point for finite values of the critical field, where the phase transition changes from first to second order.

Our study will be done numerically by using standard finite-size scaling [7] to obtain the phase diagram of the models, and the machinery arising from conformal invariance [8, 9] to distinguish the several possible critical behaviours. In the location of multicritical points for $Q > 4$ we also perform some Monte Carlo simulations by calculating the fourth-order cumulant of the magnetization.

2. The model

Defining at each lattice site $\vec{r} = (i, j)$ of a square lattice an integer variable $n_{\vec{r}} = 0, 1, \ldots, Q-1$, the Hamiltonian of the Q-state Potts model with n_h ($n_h = 0, 1, \ldots, Q-1$) symmetry-breaking fields $\{\tilde{h}_m\}$ ($m = 0, 1, \ldots, n_h - 1$) is given by

$$H_Q(\epsilon, \{\tilde{h}_m\}) = -\epsilon \sum_{\langle\vec{r},\vec{r}'\rangle} \delta_{n_{\vec{r}},n_{\vec{r}'}} - \sum_{m=0}^{n_h-1} \sum_{\vec{r}} \tilde{h}_m \delta_{n_{\vec{r}},m} \tag{1}$$

where $\epsilon > 0$ is the ferromagnetic coupling and the first sum runs over nearest-neighbour sites. In the absence of external fields the model has a $Z(Q)$ symmetry, since the configuration $\{n_{\vec{r}}\}$ and $\{n_{\vec{r}} + l, \mathrm{mod} Q\}$ ($l = 1, 2, \ldots, Q$) has the same energy. The fields $\{\tilde{h}_m\}$, depending on their relative values, break this symmetry totally or partially. The interesting cases where the symmetry is partially broken are those where $\tilde{h}_m = \tilde{h} > 0$ ($m = 0, 1, \ldots, n_h - 1$) and the remaining symmetry is $Z(n_h) \otimes Z(Q - n_h)$. This symmetry corresponds to $Z(n_h)$ rotations among the variables pointing in the field directions and $Z(Q - n_h)$ rotations among the other variables. At zero temperature we have n_h ground states and we do expect that the $Z(n_h)$ symmetry is spontaneously broken.

Rather than working with the above Euclidean version of the model it is convenient to consider its quantum Hamiltonian version in order to simplify our numerical analysis. As usual [10] both versions are expected to share the same long-distance physics since the vertical–horizontal anisotropy in the coupling constants does not destroy the essential physical ingredients of the model. The row-to-row transfer matrix as well as the associated τ-continuum quantum Hamiltonian [10] can be derived by a standard procedure (see [11] for example). The associated one-dimensional quantum Hamiltonian in an L-site chain is given by

$$\hat{H} = -\sum_{l=1}^{L} \sum_{\alpha=0}^{q-1} \left((\hat{S}_l \hat{S}_{l+1}^\dagger)^\alpha + \lambda \hat{R}_l^\alpha + \sum_{m=0}^{n_h-1} h_m (\hat{S}_l \, \mathrm{e}^{-(2\pi \mathrm{i}/Q)m})^\alpha \right) \tag{2}$$

where λ plays the role of temperature and the magnetic fields $\{h_m\}$ ($m = 0, 1, \ldots, n_h - 1$) are related with the fields $\{\tilde{h}_m\}$ in (1). In equation (2) $\hat{S}_l$ and $\hat{R}_l$ are $L^Q \otimes L^Q$ matrices satisfying the $Z(Q)$ algebra

$$[\hat{R}_l, \hat{S}_k] = (\theta - 1)\delta_{k,l} \hat{S}_k \hat{R}_l \qquad \hat{R}_l^q = \hat{S}_l^q = 1$$

where $\theta = \exp(\mathrm{i}2\pi/Q)$, and in the basis where $\hat{S}_l$ is diagonal they are given by

$$\hat{S}_l = 1 \otimes 1 \otimes \cdots 1 \otimes S \otimes 1 \cdots \otimes 1$$
$$\hat{R}_l = 1 \otimes 1 \otimes \cdots 1 \otimes R \otimes 1 \cdots \otimes 1$$

where the matrices S and R are in the lth position in the product and are given by

$$S = \sum_{i=0}^{Q-1} \theta^i |i\rangle\langle i| \qquad R = \sum_{i=0}^{Q-1} |i\rangle\langle [i+1]_Q|$$

and the symbol $[x+y]_Q$ means the addition $(x+y)$, modulo Q.

In the absence of magnetic fields ($h_m = 0$; $m = 0, 1, \ldots, n_h - 1$) the $Z(Q)$ symmetry of (1) is reflected in (2) by its commutation with the $Z(Q)$-charge operator

$$\hat{P} = \prod_{i=1}^{L} \hat{R}_l \qquad \hat{P}^Q = 1\,. \tag{3}$$

The Hilbert space associated with (2) can therefore be separated into disjoint sectors labelled by the eigenvalues $\exp(\mathrm{i}2\pi q/Q)$, ($q = 0, 1, \ldots, Q-1$) of (3). The interesting cases, which we will concentrate on in this paper, are obtained by choosing in (2) equal values for the magnetic fields†

$$h_1 = h_2 = \cdots = h_{n_h} = h > 0\,. \tag{4}$$

In this case the symmetry $Z(n_h) \otimes Z(Q - n_h)$ of (1) is reflected by the simultaneous commutation of (2) with the 'parity' operators

$$\hat{V} = \prod_{i=1}^{L} \hat{V}_l \qquad \hat{V}^{n_h} = 1 \tag{5}$$

$$\hat{W} = \prod_{i=1}^{L} \hat{W}_l \qquad \hat{W}^{Q-n_h} = 1 \tag{6}$$

with

$$\hat{V}_l = 1 \otimes 1 \otimes \cdots 1 \otimes V \otimes 1 \cdots \otimes 1$$
$$\hat{W}_l = 1 \otimes 1 \otimes \cdots 1 \otimes W \otimes 1 \cdots \otimes 1$$

and V and W, located at the lth position in the product, are $Q \times Q$ matrices given by

$$V = \sum_{i=0}^{n_h-1} |i\rangle\langle [i+1]_{n_h}| + \sum_{i=n_h}^{Q-1} |i\rangle\langle i|$$
$$W = \sum_{i=0}^{n_h-1} |i\rangle\langle i| + \sum_{i=n_h}^{Q-1} |i\rangle\langle [i+1]_{Q-n_h}|\,.$$

The Hilbert space associated with (2) is now separated into $n_h(Q - n_h)$ disjoint sectors labelled by the eigenvalues $\exp(\mathrm{i}2\pi v/n_h)$ and $\exp(\mathrm{i}2\pi w/Q - n_h)$ ($v = 0, 1, \ldots, n_h - 1$, $w = 0, 1, \ldots, Q - n_h - 1$) of the operators $\hat{V}$ and $\hat{W}$, respectively.

In the numerical diagonalization of (2), with periodic boundaries, all the above symmetries, together with the translational invariance, enable us to handle large lattices with modest computer time and memory. We use the Lanczos method to diagonalize (2) up to $L = 10, 11$ and 13, for $Q = 5, 4$ and 3, respectively.

† The cases where $h < 0$ are physically equivalent to the choices $n'_h = Q - n_h$, with $h' > 0$.

3. Results

We considered in our study only the interesting cases where $Q > n_h \geqslant 2$ and $h_1 = h_2 = \cdots = h_{n_h} = h \geqslant 0$, since in these cases a symmetry $Z(Q')$ ($Q' = n_h \geqslant 2$) always remains for $h \neq 0$.

When $h = 0$ the model is self-dual with a phase transition at $\lambda_c(0) = 1$, which has a second-order or first-order nature depending on whether $Q \leqslant 4$ or $Q > 4$, respectively. In the limit $h \to \infty$ the eigenvectors of $\hat{S}_i$ in (2) with eigenvalues θ^l, $l = n_h, n_h+1, \ldots, Q-1$, are forbidden and we have an effective n_h-state Potts model at zero field. Analysing the effect of (2) in the remaining n_h^L-dimensional Hilbert space it is not difficult to see that the phase transition happens at

$$\lambda_c(h \to \infty) = \frac{Q}{n_h}\,. \tag{7}$$

Between these two extremum values of h we estimate the phase transition curve $\lambda_c(h)$ by using standard finite-size scaling. The curve is evaluated by extrapolations to the bulk limit ($L \to \infty$) of sequences $\lambda_c(h, L)$ obtained by solving [7]

$$\Gamma_L(\lambda_c)L = \Gamma_{L+1}(\lambda_c)(L+1) \qquad L = 2, 3 \ldots \tag{8}$$

where $\Gamma_L(\lambda_c)$ is the mass gap of the Hamiltonian (2) with L sites.

Once the transition curve is estimated, in the region of continuous phase transitions we expect the model to be conformally invariant. This symmetry allows us to infer the critical properties from the finite-size corrections to the eigenspectrum at λ_c [8]. The conformal anomaly c can be calculated from the large-L behaviour of the ground-state energy $E_0(L)$. For periodic chains $E_0(L)$ behaves as

$$\frac{E_0(L)}{L} = \epsilon_\infty - \frac{\pi c v_{\mathrm{s}}}{6L^2} + \mathrm{o}(L^{-2}) \tag{9}$$

where ϵ_∞ is the ground-state energy, per site, in the bulk limit and v_{s} is the sound velocity. The scaling dimensions of operators governing the critical fluctuations (related to critical exponents) are evaluated from the finite-L corrections of the excited states. For each primary operator, with dimension x_ϕ and spin s_ϕ, in the operator algebra of the system, there exists an infinite tower of eigenstates of the quantum Hamiltonian, whose energy $E^\phi_{m,m'}$ and momentum $P^\phi_{m,m'}$, in a periodic chain are given by

$$\begin{aligned} E^\phi_{m,m'}(L) &= E_0 + \frac{2\pi v_{\mathrm{s}}}{L}(x_\phi + m + m') + \mathrm{o}(L^{-1}) \\ P^\phi_{m,m'} &= (s_\phi + m - m')\frac{2\pi}{L} \end{aligned} \tag{10}$$

where $m, m' = 0, 1, \ldots$.

We present our results separately for the cases $Q \leqslant 4$ and $Q > 4$ in the next sections.

3.1. Models with $Q \leqslant 4$

There exist three interesting cases, namely, the three-state Potts model with two fields ($Q = 3, n_h = 2$) and the four-state Potts model with three and two fields ($Q = 4, n_h = 3, 2$).

The critical curves were obtained by solving (8) and are estimated from the spectra of lattice sizes up to $L = 11$, $L = 10$ and $L = 8$ for $Q = 3$, $Q = 4$ and $Q = 5$, respectively. As an example, in figure 1 we show the extrapolated curve for the case of $Q = 3$ and $n_h = 2$ and in table 1 we show the finite-size sequences together with the extrapolated results for some values of h. We also show in figure 1 the curve obtained by

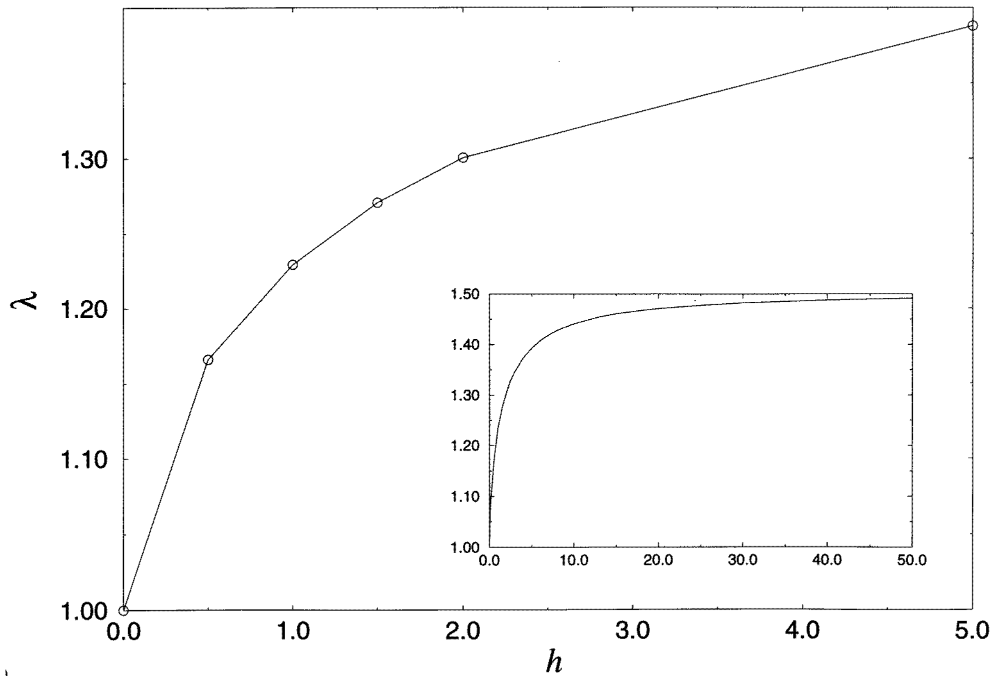

Figure 1. Estimates for the critical curve of the three-state Hamiltonian (2) with $n_h = 2$ fields. The curve in the largest scale, for $0 < h < 5$, interpolates the points obtained by extrapolating the solutions of (8) for $L = 2$–13 (circles). The inserted curve for $0 < h < 50$ was obtained by solving (8) for $L = 5$.

Table 1. Finite-size data $\lambda_c^{L-1,L}$ and extrapolations for the transition temperature of the three-state Potts chain (2) with $n_h = 2$ magnetic fields ($h_0 = h_1 = h$). These sequences are obtained by solving (8) for $L = 4$–11.

$N \backslash h$	0.5	1.0	1.5	2.0
5	1.171 942 2	1.235 993 5	1.278 124 7	1.308 620 2
6	1.168 766 4	1.232 876 8	1.274 685 7	1.304 939 5
7	1.167 567 9	1.231 445 9	1.273 072 9	1.303 209 6
8	1.166 999 4	1.230 687 4	1.272 214 6	1.302 289 4
9	1.166 684 3	1.230 246 6	1.271 715 8	1.301 754 8
10	1.166 492 0	1.229 972 8	1.271 406 1	1.301 423 1
11	1.166 367 0	1.229 793 8	1.271 203 7	1.301 206 4
∞	1.1660(4)	1.2292(8)	1.2706(2)	1.3005(9)

solving (8) for $L = 5$. We clearly see an agreement with the limiting values $\lambda_c(0) = 1$ and $\lambda_c(h \to \infty) = \frac{3}{2}$, predicted by (7). Similar curves are obtained in the other cases. In order to extract the conformal anomaly and dimensions from finite-lattice data and relations (9), (10) we need to calculate the sound velocity v_s. This can be done from the difference between higher energy states associated with the same primary operator. In our calculations we estimated v_s from the lowest energy gap between the eigenstates with momentum $2\pi/L$ and zero in the sector where $v = 1$ (tables 2 and 3) or $v = 1$, $w = 0$ (table 4). The conformal anomaly and dimensions are extracted from the diagonalization of lattice sizes

Table 2. Extrapolated and conjectured results for the conformal anomaly c and anomalous dimensions $x_n(k, v)$ of the three-state Potts chain (2) with $n_h = 2$ magnetic fields ($h_0 = h_1 = h$) (see the text). The conjectured values, in parentheses, are the corresponding ones in the critical Ising model.

h	c	$x_2(0,0)$	$x_1(1,0)$	$x_1(0,1)$	$x_1(1,1)$
0.5	0.5008(7)	1.0007(3)	2.00(1)	0.125(1)	1.125(1)
	(0.5)	(1)	(2)	(0.125)	(1.125)
1.0	0.5000(0)	0.9999(6)	1.999(5)	0.1249(7)	1.1249(7)
	(0.5)	(1)	(2)	(0.125)	(1.125)
1.5	0.5000(3)	1.0000(0)	1.9999(7)	0.124(9)	1.124(9)
	(0.5)	(1)	(2)	(0.125)	(1.125)
2.0	0.5000(8)	1.0000(0)	2.0000(0)	0.1250(0)	1.1250(0)
	(0.5)	(1)	(2)	(0.125)	(1.125)

Table 3. Extrapolated and conjectured results for the conformal anomaly c and anomalous dimensions $x_n(k, v)$ of the four-state Potts chain (2) with $n_h = 3$ magnetic fields ($h_0 = h_1 = h_2 = h$) (see the text). The conjectured values, in parentheses, are the corresponding ones appearing in the three-state Potts model.

h	c	$x_2(0,0)$	$x_3(0,0)$	$x_1(0,1)$	$x_2(0,1)$	$x_1(1,1)$	$x_2(1,1)$
0.5	0.80(0)	0.800(1)	2.7(9)	0.133(3)	1.33(2)	1.133(3)	2.33(2)
	(0.8)	(0.8)	(2.8)	(0.133...)	(1.33...)	(1.13 3...)	(2.33...)
1.0	0.799(1)	0.799(7)	2.(8)	0.132(9)	1.33(0)	1.132(9)	2.33(1)
	(0.8)	(0.8)	(2.8)	(0.133...)	(1.33...)	(1.13 3...)	(2.33...)
1.5	0.7(9)	0.79(9)	2.8(3)	0.133(4)	1.33(0)	1.133(4)	2.331(9)
	(0.8)	(0.8)	(2.8)	(0.133...)	(1.33...)	(1.13 3...)	(2.33...)
2.0	0.799(1)	0.799(9)	2.8(4)	0.1334(5)	1.33(0)	1.1334(5)	2.331(9)
	(0.8)	(0.8)	(2.8)	(0.133...)	(1.33...)	(1.133...)	(2.33...)

Table 4. Extrapolated and conjectured results for the conformal anomaly c and anomalous dimensions $x_n(k, v, w)$ of the four-state Potts chain (2) with $n_h = 2$ magnetic fields ($h_0 = h_1 = h$) (see the text). The conjectured values, in parentheses, are the corresponding ones in the critical Ising model.

h	c	$x_2(0,0,0)$	$x_1(1,0,0)$	$x_1(0,1,0)$	$x_1(1,1,0)$
0.5	0.500(2)	0.99(7)	1.94(4)	0.124(8)	1.124(8)
	(0.5)	(1)	(2)	(0.125)	(1.125)
1.0	0.50(5)	1.000(0)	1.99(9)	0.1250(9)	1.1250(9)
	(0.5)	(1)	(2)	(0.125)	(1.125)
1.5	0.500(0)	0.999(9)	1.999(6)	0.124(9)	1.124(9)
	(0.5)	(1)	(2)	(0.125)	(1.125)
2.0	0.500(0)	0.999(9)	1.999(7)	0.1249(9)	1.1249(9)
	(0.5)	(1)	(2)	(0.125)	(1.125)

up to $L = 13$, $L = 11$ and $L = 10$ for $Q = 3$, $Q = 4$ and $Q = 5$, respectively. In tables 2–4 we show for some values of h the extrapolated results obtained for the cases ($Q = 3, n_h = 2$) ($Q = 4, n_h = 3$) and ($Q = 4, n_h = 2$), respectively. In these tables we also present our conjectured values. The dimensions $x_n(k, v)$ and $x_n(k, v, w)$ appearing in these tables are obtained by using in (10) the nth ($n = 1, 2, 3, \ldots$) eigenenergy in

Table 5. Finite-size data for the dimensions appearing in table 3 for $h_o = h_1 = 0.5$.

N	c	$x_2(0,0)$	$x_3(0,0)$	$x_1(0,1)$	$x_2(0,1)$	$x_1(1,1)$	$x_2(1,1)$
4	1.163 061	0.887 205	1.425 469	0.151 106	1.372 092	1.151 106	2.043 787
5	0.987 025	0.865 098	1.752 073	0.144 513	1.352 017	1.144 513	2.129 591
6	0.916 140	0.850 707	2.044 138	0.141 080	1.343 087	1.141 080	2.182 175
7	0.879 673	0.841 268	2.309 421	0.139 052	1.338 565	1.139 052	2.216 561
8	0.858 147	0.834 729	2.526 251	0.137 749	1.336 066	1.137 749	2.240 261
9	0.844 289	0.829 975	2.658 683	0.136 862	1.334 600	1.136 862	2.257 301
10	0.834 816	0.826 382	2.721 638	0.136 230	1.333 701	1.136 230	2.269 973
11	0.828 048	0.823 581	2.752 943	0.135 765	1.333 134	1.135 765	2.279 661
∞	0.80(0)	0.800(1)	2.7(9)	0.133(3)	1.33(2)	1.133(3)	2.33(2)

the sector with momentum $2\pi k/L$ ($k = 0, 1, \ldots$) and eigenvalues $\exp(i2\pi v/Q - n_h)$ and $\exp(i2\pi w/Q - n_h)(v = 0, 1, \ldots, n_h - 1,\ w = 0, 1, \ldots, Q - n_h - 1)$ of the operators $\hat{V}$ and $\hat{W}$ defined in (5) and (6), respectively. The ground-state energy is the first energy ($n = 1$) in the sector with ($k = 0, v = 0$) in the cases ($Q = 3, n_h = 2$), ($Q = 4, n_h = 3$) and in the sector ($k = 0, v = 0, w = 0$) in the case ($Q = 4$, $n_h = 2$). The extrapolations were obtained by using the ϵ-alternated VBS approximants [12]. The errors are estimated from the stability of the extrapolations and are in the last digit. In order to illustrate these we also show in table 5 the finite-size sequences used to estimate the dimensions in the case where $Q = 3$, $n_h = 2$ and $h = 0.5$.

We see in table 2 that for all values of h the conformal anomaly is $c = \frac{1}{2}$, indicating that the model shares the same universality class as the $Z(2)$ Ising model. The dimensions 1 and $\frac{1}{8}$ correspond to the dimensions of the energy and magnetic operator in the Ising model and the dimension $2 = 1 + 1$ and $\frac{9}{8} = 1 + \frac{1}{8}$ are the next dimensions in the tower of these operators (see equation (10)).

In table 3 we clearly see that the conformal anomaly for all values of h is $c = \frac{4}{5}$. There exist two modular invariant universality classes of conformal theories with $c = \frac{4}{5}$ [13]. One of these can be represented by the restricted solid-on-solid (RSOS) model [16, 17] and the other by the three-state Potts model with no magnetic fields. These two models, although having the same conformal anomaly $c = \frac{4}{5}$, have a distinct operator content. The dimension $x = 0, \frac{4}{5}, \frac{14}{5}, \frac{2}{5}, \frac{4}{3}$ in table 3 and the degeneracy of the sectors where the operator $\hat{V}$ in (5) has eigenvalues $\exp(i2\pi/3)$ and $\exp(i4\pi/3)$ indicate that the model belongs to the same universality class as the three-state Potts model.

In table 4, as in table 2, the conformal anomaly is $c = \frac{1}{2}$ and the dimensions are those of the Ising model indicating that both models are in the same universality class.

Beyond the values of h presented in tables 1–3 we also performed a careful analysis for small values of ($h \sim 0.01$) finding similar results to those presented in these tables. These indicate that for $Q \leqslant 4$, where the model has a second-order phase transition in the absence of external fields, the introduction of n_h ($Q > n_h \geqslant 2$) fields, of arbitrary strength, brings the model into the universality class of a Potts model with n_h states.

3.2. *Models with $Q > 4$*

In this case, while in the absence of external fields the models exhibit a first-order phase transition the introduction of n_h magnetic fields ($4 \geqslant n_h \geqslant 2$) of infinite and equal strength ($h \to \infty$) render them an effective n_h-state Potts model, which has a second-order phase transition. This brings the interesting possibility of a multicritical behaviour for a finite value of h, when the transition curve changes from second to first order as we decrease h from the infinite value. In fact, this is the mean-field prediction [6].

Table 6. Finite-size sequences $c_{L,L+1}$, defined in (9) for the five-state Potts model Hamiltonian (2) with $n_h = 2$ ($h_0 = h_1 = h$) external magnetic fields. The last line gives the extrapolated results. These sequences are calculated at the extrapolated couplings $\lambda_c = 1.067(3)$, $\lambda_c = 1.113(7)$, $\lambda_c = 1.333(8)$ and $\lambda_c = 1.500(1)$ for $h = 0.05$, $h = 0.1$, $h = 0.5$ and $h = 1.0$, respectively.

$N \setminus h$	0.05	0.1	0.5	1.0
4	1.494 578	1.293 239	0.822 347	0.747 102
5	1.150 201	0.947 010	0.665 147	0.632 826
6	0.957 555	0.784 083	0.603 697	0.583 638
7	0.834 717	0.696 948	0.572 906	0.558 058
8	0.753 559	0.646 537	0.554 626	0.542 796
9	0.698 775	0.615 352	0.542 598	0.532 888
10	0.660 931	0.594 802	0.534 149	0.526 071
∞	0.5(7)	0.5(5)	0.48(9)	0.50(0)

Since the Hilbert space grows exponentially with Q, the simplest case where the above critical point may occur is the five-state Potts model in the presence of $n_h = 2$ magnetic fields. In table 6 we present, for some values of h, our results for the finite-size sequences of the conformal anomaly of the model. These sequences are obtained from (10) and (9)

$$c_{L,L+1} = \frac{12[(L+1)E_0(L) - LE_0(L+1)]}{[(L+1)^2 - L^2][E_2(L+1) - E_1(L+1)]} \tag{11}$$

where $E_0(L)$ is the ground-state energy for the chain of length L and $E_2(L)$, $E_1(L)$ are the lowest eigenenergies with momentum 0 and $2\pi/L$, respectively, in the sector where the operators $\hat{V}$ and $\hat{W}$, defined in (5) and (6) has eigenvalues (-1) and (1). Although the precision is lower than those of the preceding tables these results indicate that for $h \gtrsim 0.05$ we still have an Ising-like behaviour with $c = \frac{1}{2}$. For $h < 0.05$, and for the lattice sizes we were able to handle, it is not possible to obtain reliable results using (11).

A heuristic method, which was proved to be effective in obtaining multicritical points in earlier works [16] is to simultaneously solve (8) for three different lattice sizes

$$\Gamma_L(\lambda_c)L = \Gamma_{L+1}(\lambda_c)(L+1) = \Gamma_{L+2}(\lambda_c)(L+2)\,. \tag{12}$$

We tried to solve these equations for $0.5 > \lambda > 0$ ($L = 5$) and found no consistent solutions, which indicates the absence of a tricritical point for a finite value of h.

Another method, also used to locate multicritical points [16], is obtained from the simultaneous crossing of two different gaps on a given pair of lattices (instead of three lattices as in (12)). Trying several different gaps we also did not find, within this method, a multicritical point for $h \neq 0$.

Since these methods are heuristic and the lattice sizes we are considering may not be enough to obtain the bulk limit ($L \to \infty$) in the region $h \sim 0$ we will supplement our results by Monte Carlo simulations. These simulations will enable us to distinguish the order of the phase transition as we change the magnetic field strength. We simulate the systems by the heat-bath algorithm and analyse the fourth-order cumulant of the magnetization as a function of the magnetic field. The simulations were done directly in the classical version of the model (1). Since the evidence of a multicritical point, for non-zero values of h,

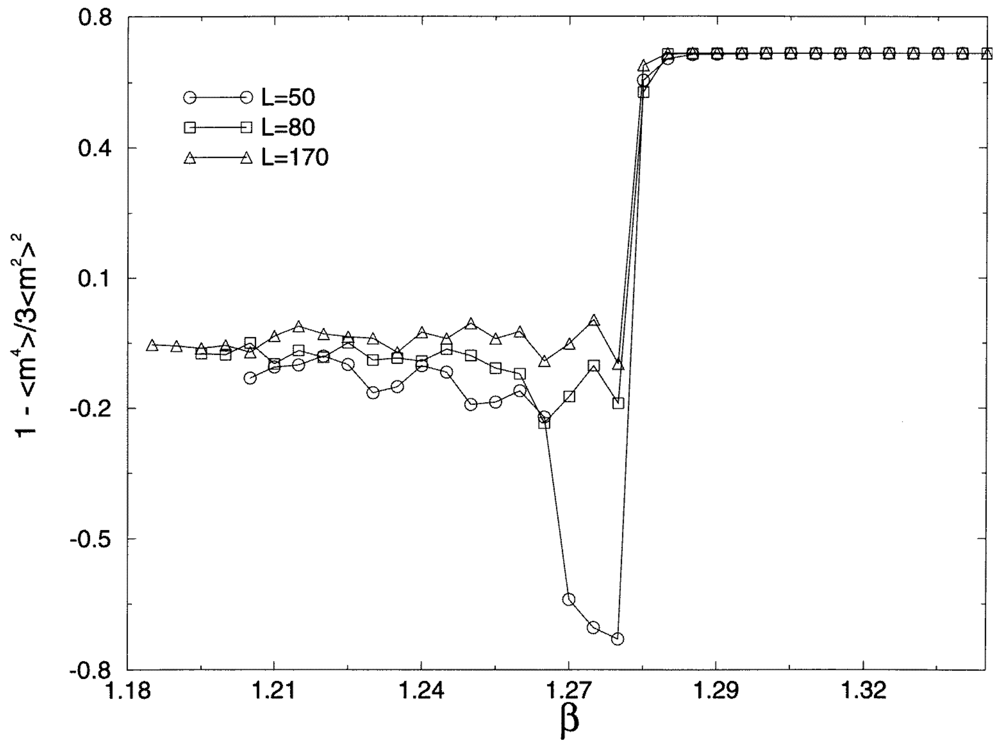

Figure 2. Fourth-order cumulant of the magnetization (13) as a function of β for the seven-state Potts model in the presence of $n_h = 2$ external fields $\tilde{h}_0 = \tilde{h}_1$=0.01 (see equation (1)). The lattice sizes are $L = 50 \times 50$, $L = 80 \times 80$ and $L = 170 \times 170$.

would be large for higher values of Q, we choose $Q = 7$ and $n_h = 2$ ($\tilde{h}_0 = \tilde{h}_1 = h$) for extensive calculations.

The fourth-order cumulant of the magnetization is defined by

$$U_L = 1 - \frac{\langle m^4 \rangle_L}{3\langle m^2 \rangle_L^2} \tag{13}$$

where the averages are done on an $L \times L$ lattice. The magnetization in (13), for a given configuration $\{n_{\vec{r}}\}$ of classical variables, is defined by

$$m = \frac{1}{L^2} \sum_{\vec{r}} (\delta_{n_{\vec{r}},0} - \delta_{\vec{r},1}) \, .$$

Following Binder [17], the cumulant (13) will be zero for $T > T_c$ and $U_L = \frac{2}{3}$ for $T < T_c$. At the transition temperature T_c equation (13) will be zero for continuous phase transitions and negative for first-order phase transitions.

In figure 2 we show the values of U_L for lattice sizes $50 \times 50, 80 \times 80$ and 170×170. In the simulations we choose $\epsilon = 1$, $\tilde{h} = 0.01$ and each point was obtained by averaging 5×10^4 iterations, after thermalization. We see in this figure that while for $L = 50$ the phase transition appears to be first order, as L grows the numerical results indicates the phase transition to be continuous. The result for the smaller lattice $L = 50$ is clearly due to the finite size of the lattice. By repeating these simulations for even smaller values of $\tilde{h}$

we should expect that these finite-size effects will be apparent for even larger lattices, and our simulations are in favour of a multicritical point only at $\tilde{h} = 0$.

4. Conclusion

We have calculated the phase transition diagram and critical properties of the Q-state Potts model in the presence of n_h $(Q > n_h > 1)$ external magnetic fields of equal strength $h > 0$. In the case where $Q > n_h \geqslant 2$ the original symmetry, at $h = 0$, breaks into a $Z(n_h) \otimes Z(Q - n_h)$ symmetry. The $Z(n_h)$ part of the above symmetry relates the configurations of the n_h distinct ground-state configurations at zero temperature, and by standard arguments, should be spontaneously broken at low temperatures.

Our results, based on conformal invariance and supplemented by Monte Carlo simulation indicate that, for arbitrary values of h, the order–disorder phase transition associated with the global $Z(n_h)$ symmetry is in the same universality class of the n_h-state Potts model. Moreover, for $Q > 4$, contrary to the mean-field prediction, we do not see any evidence of a multicritical point for non-zero values of h. This is a surprising and quite unusual result since the presence of equal $4 \geqslant n_h \geqslant 2$ arbitrary small symmetry-breaking fields in the $Q > 4$ models, which in the absence of fields have finite gap and correlation length at the transition point, will produce effective n_h-state Potts models with no gap and infinite correlation length. Certainly additional calculations using different methods or even more extended calculations will be welcome to test our available evidence in favour of the above scenario.

Acknowledgments

We thank M T Batchelor for a careful reading of our manuscript. This work was supported in part by Conselho Nacional de Desenvolvimento Científico e Tecnológico—CNPq-Brazil and by Fundação de Amparo à Pesquisa do Estado de São Paulo-FAPESP-Brasil.

References

[1] Wu F 1982 *Rev. Mod. Phys.* **54** 235
[2] Baxter R J 1982 *Exactly Solved Models in Statistical Mechanics* (New York: Academic)
[3] von Gehlen G, Rittenberg V and Ruegg H 1986 *J. Phys. A: Math. Gen.* **19** 107; see also [7] and [13]
[4] Frölich J and Lieb E H 1979 *Commun. Math. Phys.* **60** 2338
[5] Lawrie I D and Sarbach S 1984 *Phase Transitions and Critical Phenomena* vol 9 ed C Domb and J L Lebowitz (New York: Academic) p 1
Knobler C M and Scott R L 1984 *Phase Transitions and Critical Phenomena* vol 9 ed C Domb and J L Lebowitz (New York: Academic) p 164
[6] Straley J P and Fisher M E 1973 *J. Phys. A: Math. Gen.* **6** 1310
[7] Barber M N (1983) *Phase Transitions and Critical Phenomena* vol 8 ed C Domb and J L Lebowitz (New York: Academic) p 145
[8] Cardy J L 1987 *Phase Transitions and Critical Phenomena* vol 11 ed C Domb and J L Lebowitz (New York: Academic) p 55
[9] Blöte H W J, Cardy J L and Nightingale M P 1986 *Phys. Rev. Lett.* **56** 742
Affleck I 1986 *Phys. Rev. Lett.* **56** 746
[10] Fradkin E and Susskind L 1978 *Phys. Rev.* D **17** 2637
[11] Alcaraz F C and Köberle R 1981 *J. Phys. A: Math. Gen.* **14** 1169
[12] van den Broeck J M and Swartz L W 1979 *SIAM J. Math. Anal.* **10** 658
Hamer C J and Barber M N 1981 *J. Phys. A: Math. Gen.* **14** 2009
[13] Cappelli A, Itzykson C and Zuber J-B 1987 *Nucl. Phys.* B **280** 445; 1987 *Commun. Math. Phys.* **113** 1
[14] Andrews E, Baxter R J and Forrester P J 1984 *J. Stat. Phys.* **35** 193

[15] Huse D A 1984 *Phys. Rev.* B **30** 3908
[16] Fisher M E and Berker N 1982 *Phys. Rev.* **26** 2707
Rikvold P A, Kinzel W, Gunton J D and Kaski K 1983 *Phys. Rev.* B **28** 2686
Hermann H J 1984 *Phys. Lett.* **100A** 156
Alcaraz F C, de Felício J R D, Köberle R and Stilck J F 1985 *Phys. Rev.* B **32** 11
Malvezzi A L 1994 *Braz. J. Phys.* **24** 2
[17] Binder K 1981 *Phys. Rev. Lett.* **47** 693; 1981 *Z. Phys.* B **43** 119
Binder K and Landau L P 1984 *Phys. Rev.* B **30** 1477